

Rényi entropy of a line in two-dimensional Ising models

J.-M. Stéphan, G. Misguich, and V. Pasquier

Institut de Physique Théorique (IPhT), CEA, CNRS, URA 2306, F-91191 Gif-sur-Yvette, France

(Received 5 July 2010; published 30 September 2010)

We consider the two-dimensional Ising model on an infinitely long cylinder and study the probabilities p_i to observe a given spin configuration i along a circular section of the cylinder. These probabilities also occur as eigenvalues of reduced density matrices in some Rokhsar-Kivelson wave functions. We analyze the subleading constant to the Rényi entropy $R_n = 1/(1-n)\ln(\sum_i p_i^n)$ and discuss its scaling properties at the critical point. Studying three different microscopic realizations, we provide numerical evidence that it is universal and behaves in a steplike fashion as a function of n with a discontinuity at the Shannon point $n=1$. As a consequence, a field theoretical argument based on the replica trick would fail to give the correct value at this point. We nevertheless compute it numerically with high precision. Two other values of the Rényi parameter are of special interest: $n=1/2$ and $n=\infty$ are related in a simple way to the Affleck-Ludwig boundary entropies associated to free and fixed boundary conditions, respectively.

DOI: [10.1103/PhysRevB.82.125455](https://doi.org/10.1103/PhysRevB.82.125455)

PACS number(s): 05.70.Jk, 05.50.+q, 75.40.Mg, 03.67.Mn

I. INTRODUCTION

The entanglement (or Von Neumann) entropy is, in general, a difficult quantity to compute in two-dimensional (2D) quantum lattice models.¹ In Ref. 2 it was, however, shown that for a particular type of wave functions, of type dubbed ‘‘Rokhsar-Kivelson’’ (RK), and for particular geometries, the calculation simplifies considerably. A lattice model of statistical mechanics can be used to define a Rokhsar-Kivelson wave function as follows:^{3,4}

$$|\text{RK}\rangle = \frac{1}{\sqrt{\mathcal{Z}}} \sum_c e^{-1/2E(c)} |c\rangle, \quad (1)$$

where the sum runs over the classical configurations and $E(c)$ is the energy associated to c (interactions are assumed to be short ranged), and the normalization factor involves the classical partition function \mathcal{Z} . For such a state, it has been shown in Ref. 5 that the eigenvalues of the reduced density matrix of a semi-infinite cylinder (with a finite circumference L , see Fig. 1) are simply the classical probabilities p_i to observe a given configuration i at the boundary between A and B . In turn, these probabilities can be obtained from the dominant eigenvector of the transfer matrix of the classical model. So, the complete entanglement spectrum is encoded in the dominant eigenvector of the classical transfer matrix.⁶ In this work, we concentrate on the situation where the classical model is a two-dimensional Ising model. Each probability p_i is therefore associated to a given configuration i of the spins along the ‘‘ring’’ of length L which separates the regions A and B (Fig. 1). Specifically, we are interested in the behavior of the Rényi entropies

$$R_{n>0} = \frac{\ln(Z_n)}{1-n} \quad Z_n = \sum_i p_i^n, \quad (2)$$

including its limit

$$\lim_{n \rightarrow 1} R_n = - \sum_i p_i \ln(p_i), \quad (3)$$

which is the Shannon entropy (or Von Neumann in the quantum/RK point of view⁵).

As discussed in previous studies,^{5,7,8} $R_n(T, L)$ scales linearly with perimeter L of the cylinder, even at the critical temperature. However, the most interesting piece of information is the first *subleading* correction, $r_n(T)$. For a given temperature T , the latter is defined through an expansion of $R_n(T, L)$ for large L

$$R_n(T, L) \simeq a_n(T)L + r_n(T) + o(1) \quad (4)$$

and is of order 1.⁹ Contrary to the coefficient a_n , r_n has been argued to be universal. In the case of Ising models, $r_1(T > T_c) = 0$ in the high-temperature phase and $r_1(T < T_c) = \ln(2)$ in the low-temperature phase.⁵ At the critical point, the previous numerical calculations (up to $L=36$) lead to $r_1(T=T_c) \simeq 0.2544$.¹⁰ The numerical results presented in Sec. II significantly increase the precision on this number: $r_1(T_c) = 0.2543925(5)$. Furthermore, we confirm its universal character by checking the agreement between three microscopically different realizations of the 2D critical Ising models: on the square and triangular lattices, and using the Ising

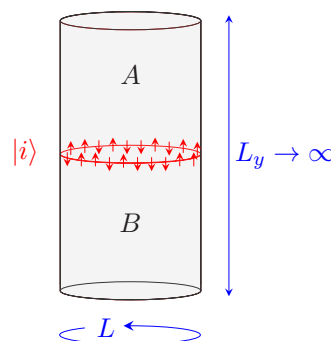


FIG. 1. (Color online) Cylinder geometry with $L_y \gg L$. A probability p_i is associated to each spin configuration i of the boundary (red circle) between A and B .

chain in transverse field (ICTF). At present, we are not aware of any field-theory method which is able to compute this number.

In Sec. III we analyze the finite-size scaling of $r_1(\mu, L)$ in the vicinity of the critical point, using numerical (but exact) calculations for the ICTF. There, the parameter μ measures the ratio of the spin-spin interaction over the strength of the external magnetic field and plays the role of the temperature in the classical Ising model. Away from $\mu = \mu_c$, we conclude that $r_1(\mu, L)$ only depends on $L(\mu - 1)$ in the critical regime, which is consistent with a correlation length diverging as $1/(\mu - 1)$ close to the critical point (located at $\mu_c = 1$). In particular, we confirm the steplike shape of $r_1(\mu, L = \infty)$.

In Sec. IV we analyze the finite-size scaling of $r_n(\mu = \mu_c = 1, L)$ in the vicinity of $n = 1/2$ and $n = 1$, again with the ICTF (up to $L = 44$ sites). The case $n = 1/2$ turns out to be exactly solvable (Sec. IV B) and related to the “ground-state degeneracy” for a critical Ising model with free boundary conditions, as discussed by Affleck and Ludwig.¹¹ In the vicinity of $n = 1$ the numerical data strongly suggests a steplike shape of $r_n(\mu = 1, L = \infty)$ as a function of the Rényi parameter n : $r_n(\mu = 1, L = \infty) = 0$ for $n < 1$ and $r_n(\mu = 1, L = \infty) = \ln 2$ for $n > 1$. This result has some important consequence regarding possible field-theory approaches. In particular, a singularity at $n = 1$ would invalidate any attempt to compute r_1 from a naive analytical continuation to $n = 1$ of the $n \in \mathbb{N}^*$ result (replica trick).

II. SHANNON ENTROPY AT THE CRITICAL POINT

A. Square and triangular lattices

We compute the Shannon entropy R_1 using the transfer matrix \mathcal{T} of the ferromagnetic Ising model. We numerically diagonalize \mathcal{T} (in the full space of dimension 2^L), on the square and on the triangular lattices¹² for sizes up to $L = 14$ and denote by $|L\rangle$ and $|E\rangle$ the left- and right-dominant eigenvectors of \mathcal{T} (corresponding to the eigenvalue with the largest modulus). Then, the probability p_i of a configuration i is given by

$$p_i = \frac{\langle L|i\rangle\langle i|R\rangle}{\langle L|R\rangle} \quad (5)$$

in the limit of a infinitely long cylinder $L_y \gg L$.

The results for $R_1(T_c)$, obtained by summing over the 2^L configurations, are shown in Fig. 2. The linear behavior, $R_1(T_c) \sim L$ is apparent, as well as the fact that the data for the two lattices extrapolate to the same value ≈ 0.254 at $L = 0$. Although the systems are relatively small, it shows that $r_1(T_c) \approx 0.254$ does not depend on the microscopic lattice geometry and is therefore very likely to be *universal*.

B. Ising chain in transverse field

As a third microscopic realization of the Ising 2D universal class, we study the ICTF

$$\mathcal{H} = -\mu \sum_{j=0}^{L-1} \sigma_j^x \sigma_{j+1}^x - \sum_{j=0}^{L-1} \sigma_j^z. \quad (6)$$

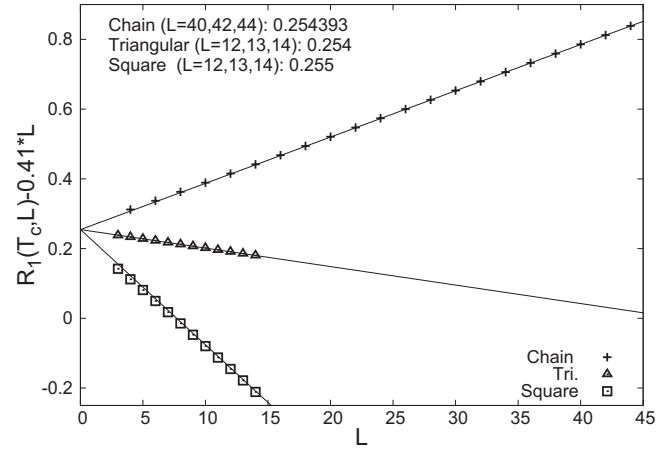


FIG. 2. Shannon entropy $R_1(T_c, L)$ of the Ising models at the critical point, plotted as a function of L (a linear term, $-0.41L$, has been subtracted for clarity). Data for the square and triangular lattices and for the Ising chain in transverse field are compared. The data are well reproduced by $R_1(L) \approx aL + r_1 + b/L$ and the subleading constant r_1 is evaluated using the three largest sizes. Each line represents the leading term and the constant, $aL + r_1$. The subleading term appears to be the same $r_1 \approx 0.254$ for the three microscopic models.

This Hamiltonian proportional to the logarithm of the transfer matrix of an anisotropic Ising model on the square lattice with couplings along the y direction (“time”) which are much stronger than in the x direction (“space”).

This Hamiltonian is transformed into a free-fermion problem using the standard Jordan-Wigner transformation. The later free-fermion problem is then diagonalized using a Bogoliubov transformation. The ground state of \mathcal{H} is then described as the vacuum of the Bogoliubov fermions. The critical point is located at $\mu = 1$. For $\mu > 1$ the system is in the ordered phase with spontaneously broken \mathbb{Z}_2 symmetry ($\langle \sigma^x \rangle \neq 0$) and for $\mu < 1$ the system is in the disordered (paramagnetic) phase.

It turns out that the ground state $|G\rangle$ of the chain is simpler to express in σ^z basis. For an Ising spin configuration $|i\rangle$ labeled by the variables $\sigma_i^z = \pm 1$, the probability at $\mu = 1$ is

$$p_i = |\langle i|G\rangle|^2 = p(\sigma_0^z, \dots, \sigma_{L-1}^z) = \det M, \quad (7)$$

where M is an $L \times L$ matrix defined by

$$M_{j\ell} = \frac{1}{2} \delta_{j\ell} + \frac{(-1)^{j-\ell} \sigma_j^z}{2L \sin \left[\pi \left(j - \ell + \frac{1}{2} \right) / L \right]}. \quad (8)$$

This result is derived in Appendix, where the noncritical case $\mu \neq 1$ is also considered. However, going back to the initial 2D classical model, the actual spin directions are measured by σ_i^x . So, we first compute an entropy $R_n^{(z)}$ corresponding to probabilities of z -axis configurations, and then use the Kramers-Wannier duality transformation¹³ to obtain the desired $R_n = R_n^{(x)}$

$$R_n^{(x)}(\mu) = R_n^{(z)}(1/\mu) + \ln 2. \quad (9)$$

TABLE I. Shannon entropy $R_1(L, \mu=1)$ of the critical Ising chain in transverse field as a function of the system size L . The subleading constant r_1 is extracted using three different fits: $r_1^{(1)}$ is obtained by a fit to $R_1(L) \approx aL + r_1 + bL^{-1}$ using the three following system sizes: $L, L-2, L-4$. $r_1^{(4)}$ is obtained by a fit to $R_1(L) \approx aL + r_1 + bL^{-1} + \dots + eL^{-4}$ using the six system sizes $L, L-2, \dots, L-10$. $r_1^{(5)}$ is obtained by a fit to $R_1(L) \approx aL + r_1 + bL^{-1} + \dots + fL^{-5}$ using the seven system sizes $L, L-2, \dots, L-12$. a is the coefficient of the extensive (and nonuniversal) term, extracted from the seven-point fit above. From this analysis, our best estimate for $L=\infty$ is $r_1=0.2543925(5)$.

L	$R_1(L)$	a_1	$r_1^{(1)}$	$r_1^{(4)}$	$r_1^{(5)}$
16	7.02789845748593	0.4232735600	0.2544012149	0.2543924985	0.2543925471
18	7.87432026832476	0.4232735603	0.2543983072	0.2543925177	0.2543925302
20	8.72076710746883	0.4232735604	0.2543965648	0.2543925180	0.2543925183
22	9.56723215961776	0.4232735605	0.2543954570	0.2543925156	0.2543925130
24	10.4137108773778	0.4232735605	0.2543947190	0.2543925136	0.2543925110
26	11.2602001105626	0.4232735606	0.2543942083	0.2543925110	0.2543925072
28	12.1066976079502	0.4232735605	0.2543938437	0.2543925139	0.2543925188
30	12.9532017180203	0.4232735608	0.2543935763	0.2543925001	0.2543924741
32	13.7997112017585	0.4232735600	0.2543933760	0.2543925306	0.2543925939
34	14.6462251114521	0.4232735614	0.2543932227	0.2543924796	0.2543923635
36	15.4927427098430	0.4232735597	0.2543931036	0.2543925326	0.2543926640
38	16.3392634147881	0.4232735610	0.2543930095	0.2543925037	0.2543924262
40	17.1857867605076	0.4232735606	0.2543929343	0.2543924999	0.2543924890
42	18.0323123698967	0.4232735603	0.2543928734	0.2543925161	0.2543925658
44	18.8788399343835	0.4232735602	0.2543928237	0.2543925300	0.2543925757

The calculation of R_n^c amounts to compute 2^L probabilities, each of which is obtained as a determinant of size $L \times L$. Using the translation invariance and the reflection symmetry of the chain, the number of probabilities to compute can be reduced to $\sim 2^L/(2L)$.¹⁴ To do so we generate one representative for each orbit of spin configurations (under the action of the lattice symmetries) using the “bracelets” enumeration algorithm of Ref. 15. For the largest size, $L=44$, computing all the probabilities ($2^L=1.7 \times 10^{13}$) required about 1000 h of CPU time on a parallel machine.

The data for the Shannon entropy R_1 are plotted in Fig. 2 and given in Table I. They significantly extend the results published in Ref. 5. The columns $r_1^{(1)}$, $r_1^{(4)}$, and $r_1^{(5)}$ correspond to three different ways to extract the subleading constant from $R_1(\mu=1, L)$ with three different types of fits (details in the table caption). In all cases the result rapidly converges and, using the largest size ($L=44$ spins) we estimate that $r_1=0.2543925(5)$ at $L=\infty$.

III. μ AWAY FROM THE CRITICAL POINT

In this section, we investigate the behavior of r_1 in the vicinity of the critical point, by considering the Ising chain in transverse field away from $\mu=1$. The results are summarized in Fig. 3.

In this plot, $r_1(\mu)$ is extracted from $R_1(L, \mu)$ using a fit to $a_1(\mu)L + r_1(\mu) + b_1(\mu)/L$ with three consecutive values of L . For the size we have studied (here $L \leq 38$), there is still some visible finite-size effects. In particular, the marked oscillations in the vicinity of $\mu=1$ are not converged to the $L=\infty$ limit. In fact, it is reasonable to expect the curves to gradu-

ally approach a steplike function as L increases: $r_1=0$ for $\mu < 1$ and $r_1=\ln(2)$ for $\mu > 1$.

This scenario, anticipated in Ref. 5, is corroborated by the scaling shown in the inset of Fig. 3. When plotted as a function of $(\mu-1)L$, the data for different system sizes and different values of μ collapse onto a single—and very likely universal—curve. This can be understood from the fact that the correlation length ξ of the Ising model diverges as $1/|\mu-1|$ at the transition, and if one assumes that r_1 is a function of $L/\xi(\mu)$ in the critical region. If correct, it imme-

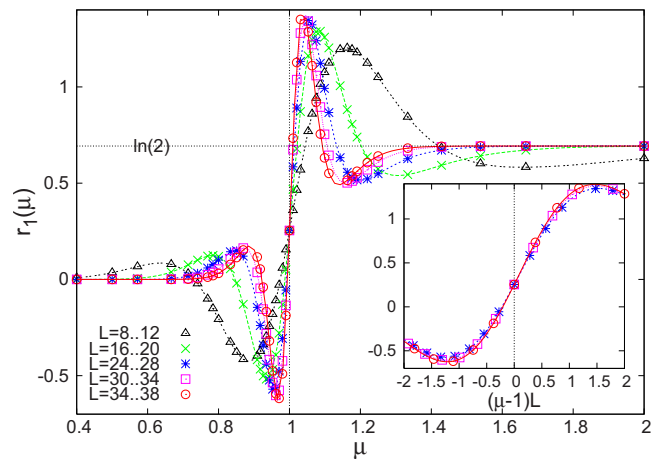


FIG. 3. (Color online) Subleading constant r_1 of the Shannon entropy of the Ising chain as a function of μ . The critical point corresponds to $\mu=1$. Inset: $r_1(\mu)$ for different system sizes, plotted as a function of $(\mu-1)L$.

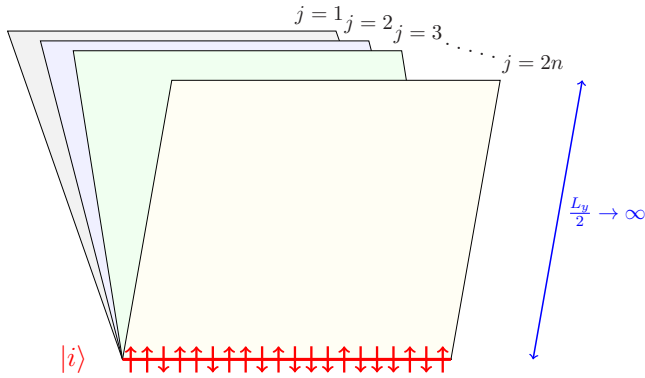


FIG. 4. (Color online) $2n$ Ising models glued together at their boundary (“Ising book”). In our case, each “page” has periodic boundary conditions along the horizontal axis and is semi-infinite in the vertical direction. Figure 1 corresponds to two pages ($n=1$).

diately implies that $r_1(\mu)$ is a steplike function in the thermodynamic limit.

IV. RÉNYI ENTROPY AWAY FROM $n=1$

We now consider the effect of changing the Rényi parameter n . When $2n$ is an integer, R_n has an interpretation in terms of the free energy of $k=2n$ semi-infinite Ising models which are “glued” together at their boundary (see Fig. 4).

Using the transfer matrix point of view, it is simple to see that $p_i^{k/2}$ is (proportional to) the probability to observe the spin configuration i on a circle along which k Ising models (defined on semi-infinite cylinders) are forced to coincide. This was used in Refs. 7 and 8 in some field-theory calculations, but it is also true at the microscopic level. The interpretation above does not apply when $2n$ is not a positive integer, but $R_n(L, \mu)$ can still be computed numerically for any $n \geq 0$.

A. Rényi parameter $n=2$ and above

When n goes to infinity, only the spin configuration with the largest probability contributes to R_n . For the ferromagnetic Ising models we consider (including the quantum chain in transverse field), this configuration is twofold degenerate and corresponds to a fully polarized ferromagnetic state, $|\uparrow\uparrow\cdots\uparrow\rangle$ or $|\downarrow\downarrow\cdots\downarrow\rangle$. In other words, taking the limit $n \rightarrow \infty$ amounts to study a semi-infinite Ising model with ferromagnetic boundary conditions. The corresponding probability, p_{\max} , behaves as $-\ln(p_{\max}) \sim aL + \ln(2)$ at the critical point.⁵ The subleading constant, $\ln(2)$, is nothing but (twice) the “ g factor” associated to this conformally invariant boundary condition (more details in Sec. IV B). This implies for the Rényi entropies that the subleading constant $r_n(\mu_c)$ is $\ln(2)$ at $n=\infty$.

In fact, for $n \geq 2$ the Fig. 5 shows that even relatively small systems give $r_n(\mu_c)$ very close to $\ln 2$. Table II is an analysis showing that $r_2(\mu=1) \approx \ln 2$ with a great accuracy, on the order of 10^{-8} . Since the convergence to $\ln 2$ is even faster when $n > 2$, there is practically no doubt that $r_n(\mu_c)$ is exactly $\ln 2$ for $n \geq 2$.¹⁶

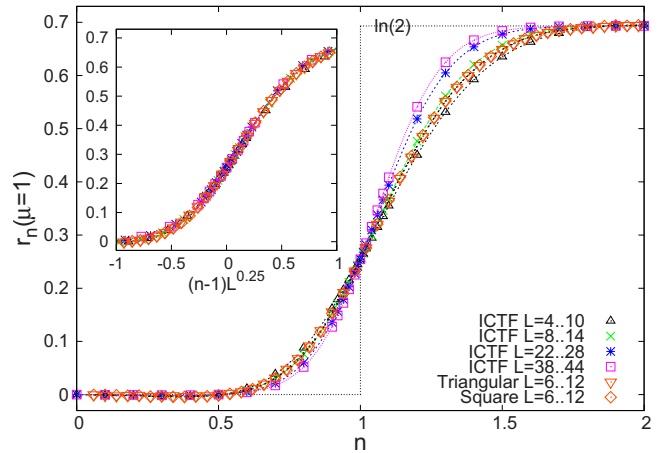


FIG. 5. (Color online) Subleading constant r_n of the Rényi entropy of the Ising chain (ICTF, at $\mu=1$) and classical Ising models (triangular and square lattice, at $T=T_c$) as a function of the Rényi parameter n . The (slow) convergence toward a step function can be observed. Inset: when plotted as a function of $(n-1)L^{0.25}$, the data collapse reasonably well onto a single curve. For each value of n , r_n is obtained by fitting the data for $R_n(L)$ to $\approx aL + r_n + bL^{-1} + cL^{-2}$ using four system size: $L, L-2, L-4$, and $L-6$, as indicated.

As a consequence, an analytical continuation of this result to $n=1$ would erroneously give $r_1(\mu_c) = \ln 2$ (instead of 0.25439). In particular, we note that the results of Ref. 8 (which use a replica technique) are in agreement with ours for $n > 1$, but not at $n=1$.

B. $n = \frac{1}{2}$

The special value $n = \frac{1}{2}$ corresponds to the free energy of a *single* Ising model defined on a semi-infinite cylinder (keeping only part A in Fig. 1) and can be treated exactly. Using the transfer matrix point of view, it is indeed simple to see that $\sqrt{p_i}$ is proportional to the probability to observe the spin configuration i at the edge of a semi-infinite Ising model (contrary to p_i which is the probability to observe i in the bulk).

As far as the universal properties are concerned, we can study the ground state of the quantum Ising chain [Eq. (6)] rather than the transfer matrix of the classical 2D model. Denoting by $|G\rangle$ the ground state of the chain, we have $\sqrt{p_i} = \langle G | i \rangle$ and the Rényi entropy $R_{1/2}$ can be written as

$$R_{1/2}(L) = 2 \ln \left(\langle G | \sum_{\{\sigma_i^z = \pm 1\}} |\sigma_1^z, \dots, \sigma_L^z\rangle \right), \quad (10)$$

$$= 2 \ln(2^{L/2} \langle G | \text{free} \rangle), \quad (11)$$

where $|\text{free}\rangle = |\{\sigma_i^z = 1\}\rangle$ is the state where all the spins point in the z direction. It turns out that the latter state is the vacuum of Jordan-Wigner Fermion and that the scalar product in Eq. (11) can be obtained as a particular case of Eqs. (7) and (8). At the critical point ($\mu=1$), the result is particularly simple⁵

TABLE II. Rényi entropy $R_2(L, \mu=1)$ of the critical Ising chain in transverse field as a function of the system size L . The subleading constant $r_2(\mu_c)$ is extracted using three different fits (same as in Table I): $r_2^{(1)}$ is obtained by a fit to $R_2(L) \approx aL + r_1 + bL^{-1}$ using the three following system sizes: $L, L-2, L-4$. $r_2^{(4)}$ is obtained by a fit to $R_2(L) \approx aL + r_1 + bL^{-1} + \dots + eL^{-4}$ using the six system sizes $L, L-2, \dots, L-10$. $r_2^{(5)}$ is obtained by a fit to $R_2(L) \approx aL + r_1 + bL^{-1} + \dots + fL^{-5}$ using the seven system sizes $L, L-2, \dots, L-12$. a is the coefficient of the extensive (and nonuniversal) term, extracted from the seven-point fit above. These data show that r_1 converges to $\ln 2$ (limit $L \rightarrow \infty$). Similar results, with an even faster convergence, show that $r_{n \geq 2}(\mu_c) = \ln(2)$. With the present systems sizes and the present machine accuracy, adding more terms in the $1/L$ expansion does not increase the accuracy on r_2 .

L	$R_2(L)$	a_2	$r_2^{(1)}/\ln 2$	$r_2^{(4)}/\ln 2$	$r_2^{(5)}/\ln 2$
20	4.95205232373074	0.2138075040	0.9989748222	0.9999928713	0.9999877126
28	6.66741530818944	0.2138074244	0.9996525352	0.9999971726	0.9999989449
36	8.38060934985332	0.2138074200	0.9998432968	0.9999991645	0.9999989996
44	10.0928119559937	0.2138074203	0.9999165184	0.9999996643	0.9999997718

$$\langle G | \text{free} \rangle = \prod_{j=0}^{L/2-1} \cos \frac{(2j+1)\pi}{4L} \quad (12)$$

and leads to the following exact expression of the $n = \frac{1}{2}$ -Rényi entropy:

$$R_{1/2}(L, \mu=1) = L \ln 2 + 2 \sum_{j=0}^{L/2-1} \ln \cos \frac{(2j+1)\pi}{4L}. \quad (13)$$

Finally, an Euler-Maclaurin expansion gives the desired finite-size scaling with a vanishing constant $r_{1/2}$

$$R_{1/2}(L, \mu=1) = a_{1/2}L + r_{1/2} + o(1), \quad (14)$$

$$a_{1/2} = \frac{2K}{\pi}, \quad (15)$$

$$r_{1/2} = 0, \quad (16)$$

where $K \approx 0.91596559$ is Catalan's constant.

The constant term in $-\ln \langle G | \text{free} \rangle$ has already been studied in Ref. 5. The situation where $|G\rangle$ is the ground state of an antiferromagnetic spin- $\frac{1}{2}$ XXZ chain has also been considered.^{5,17-21} Such a scalar product is closely related to the notion of quantum fidelity.¹⁷ In terms of a classical 2D Ising model, $-T \ln \langle G | \text{free} \rangle$ is the boundary contribution to the free energy of a semi-infinite Ising model with free boundary conditions imposed at the edge. At the critical point, this is a well-understood quantity from boundary CFT, and the subleading constant $r_{1/2}$ corresponds to $-2 \ln g$, where g is the ground-state degeneracy discussed by Affleck and Ludwig.¹¹ In the present case of the Ising model, $r_1 = 0$ is in agreement with $g_{\text{free}} = 1$.^{11,22} This result has also been checked numerically in Ref. 23.

C. Critical behavior in the vicinity of $n=1$

The results concerning the subleading constant $r_n(\mu=1)$ are summarized in Fig. 5. The behavior of $r_n(\mu=1)$ has some similarity with that of $r_1(\mu)$: the curves interpolates between 0 and $\ln 2$ with a slope at $n=1$ (respectively, $\mu=1$) which increases as a function of the system size. Here again, it

appears that the data for different values of n and L collapse onto a single curve when plotted as a function of $(n-1)L^{0.25}$ (inset of Fig. 5). The error bar on the exponent 0.25 are unfortunately large and difficult to estimate, but it indicates (a rather slow) divergence of the slope $\partial r_n / \partial n|_{n=1}$ when L increases. r_n has also been computed for the classical Ising models on the square and triangular lattices, as in Sec. II A. The inset of Fig. 5 shows that the r_n obtained from the corresponding transfer-matrix calculations are in good agreement with those calculated from the ground state of the ICTF. This is a strong indication that, in a scaling region around $n=1$, r_n defines a *universal curve*. The analogy between the effects of μ and n suggests that $n-1$ is a ‘‘relevant’’ perturbation: going slightly below (respectively, above) $n=1$ induces a drastic change in $r_n(\mu=1)$, which immediately (when $L=\infty$) goes to 0 (respectively, $\ln 2$), as in the high (respectively, low) temperature phase of the 2D Ising model.

D. Vicinity of $n=\frac{1}{2}$

The value $n=\frac{1}{2}$ can be treated exactly, as explained in Sec. IV B. However, the free-fermion calculation does not extend away from $n=\frac{1}{2}$. Still, at $n=0.5$ we observe (numerically) a crossing of the curves corresponding to different values of L (see Fig. 6). This phenomenon, also observed at $n=1$, is reminiscent of a critical behavior, where the deviation away from $n=1/2$ would play the role of an irrelevant perturbation away from a fixed point. The data can also be collapsed onto a single curve, when the y axis is multiplied by a factor $\approx L^{0.6}$. However, contrary to the case $n=1$, this result indicates a reasonably fast convergence toward $r_n=0$ in the vicinity of $n=1/2$ (see the inset of Fig. 6).

V. DISCUSSION AND CONCLUSIONS

In the present Ising models, $r_n(\mu)$ seems to take only three discrete values. For example, in the critical case, we find

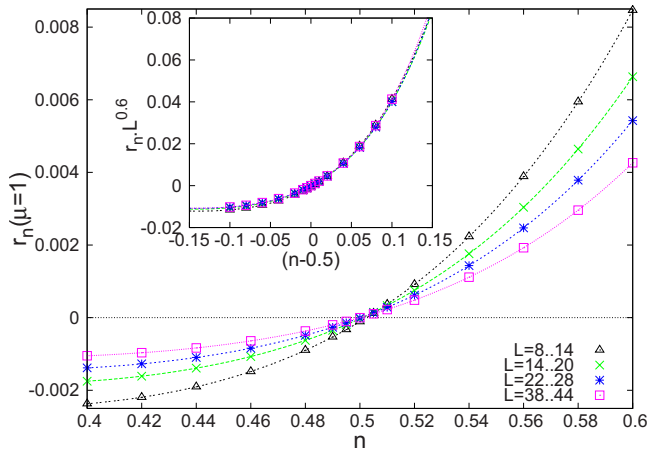


FIG. 6. (Color online) Subleading constant r_n of the Rényi entropy of the Ising chain (at the critical point $\mu=1$), in the vicinity of $n=0.5$. Inset: subleading constant multiplied by $L^{0.6}$ as a function of $(n-0.5)$.

$$r_n(\mu=1) = \begin{cases} 0, & n < 1 \\ 0.2543925(5), & n = 1 \\ \ln 2, & n > 1. \end{cases} \quad (17)$$

Similar nontrivial analytic behavior have already been reported for other models.^{24–26} This is quite different from other models described in terms of a free field compactified (with radius R) in the long-distance limit. In that case, which is better understood from a field-theory point of view, the system describes a line of fixed points and the subleading constant $r_n(R)$ continuously varies along that critical line^{27,28}

$$r_n(R) = \ln R - \frac{\ln n}{2(n-1)}. \quad (18)$$

We have discussed how the special values $n=\frac{1}{2}$ and $n=\infty$ are related to the g factors associated to free and fixed boundary conditions of the Ising model. But so far, we do not know how to understand $r_{n=1}$ for the critical Ising model using CFT. This is certainly an interesting question for future studies. Up to now, the replica trick has been a very successful tool for extracting such universal quantities, especially in one-dimensional quantum spin chains.^{29,30} However, it seems (see Secs. IV A and IV C) that this method cannot be applied to the Ising critical point for our quantity. This makes the analytical computation of $r_{n=1}$ all the more challenging. It is tempting to conjecture that crossings for $r_n(L)$ are observed whenever the underlying probabilities, $\sim p_i(\mu)^n$ describe a conformally invariant setup. It is indeed the case at $n=1/2$ (Ising boundary with free boundary conditions), but it is also realized for $n=1$, since it correspond to the bulk probabilities. We also expect that the nonanalytical behavior of r_n in the vicinity of $n=1$ could be a generic feature of all minimal models. Finally, it would be interesting to investigate possible connections with the theory of line defects in conformally invariant systems.^{31,32}

ACKNOWLEDGMENTS

We wish to thank J. Dubail, S. Furukawa, A. Läuchli, Ph. Lecheminant, M. Oshikawa, and H. Saleur for several useful discussions and suggestions. The numerical calculations were done on the machine titane at the “Centre de calcul centralisé du CEA” under the Project No. p575.

APPENDIX: PROBABILITY OF A SPIN CONFIGURATION

We consider an Ising chain in transverse field

$$\mathcal{H} = -\mu \sum_{j=0}^{L-1} \sigma_j^x \sigma_{j+1}^x - \sum_{j=0}^{L-1} \sigma_j^z. \quad (A1)$$

We assume L to be even, as well as periodic boundary conditions $\sigma_L^x = \sigma_0^x$. We wish to find the ground state $|G\rangle$ of this Hamiltonian and to compute all of his components in the basis of the eigenstates of the σ_j^z .

1. Diagonalization

As is well known, \mathcal{H} can be expressed in terms of free fermions, using the Jordan-Wigner transformation

$$\sigma_j^x + i\sigma_j^y = 2c_j^\dagger \exp\left(i\pi \sum_{l=0}^{j-1} c_l^\dagger c_l\right), \quad (A2)$$

$$\sigma_j^z = 2c_j^\dagger c_j - 1, \quad (A3)$$

where the c, c^\dagger satisfy the canonical anticommutation relations $\{c_j, c_l^\dagger\} = \delta_{j\ell}$. This allows to write the Hamiltonian as a quadratic form

$$\mathcal{H} = -\sum_{j=0}^{L-1} (2c_j^\dagger c_j - 1) - \mu \sum_{j=0}^{L-1} (c_j^\dagger - c_j)(c_{j+1}^\dagger + c_{j+1}), \quad (A4)$$

where the fermions are subject to boundary condition

$$c_L^\dagger = -\exp(i\pi\mathcal{N})c_0^\dagger, \quad \mathcal{N} = \sum_{l=0}^{L-1} c_l^\dagger c_l. \quad (A5)$$

The parity operator \mathcal{P} commutes with \mathcal{H}

$$\mathcal{P} = \prod_{j=0}^{L-1} \sigma_j^z = \exp(i\pi\mathcal{N}) = \pm 1, \quad (A6)$$

and because of Perron-Frobenius theorem, the ground state lies in the sector $\mathcal{P}=+1$. Therefore, fermions are subjected to antiperiodic boundary conditions $c_L^\dagger = -c_0^\dagger$. \mathcal{H} can finally be diagonalized by a Bogoliubov transformation

$$c_j^\dagger = \frac{1}{\sqrt{L}} \sum_k e^{ikj} (\cos \theta_k d_k - i \sin \theta_k d_{-k}^\dagger), \quad (A7)$$

$$k \in \{(2l+1)\pi/L | -L/2 \leq l \leq L/2 - 1\}, \quad (\text{A8})$$

$$\sin 2\theta_k = \frac{\mu \sin k}{\sqrt{1 + 2\mu \cos k + \mu^2}}, \quad (\text{A9})$$

$$\cos 2\theta_k = \frac{1 + \mu \cos k}{\sqrt{1 + 2\mu \cos k + \mu^2}}. \quad (\text{A10})$$

The new fermions operators d_k, d_k^\dagger satisfy the necessary anticommutation relations and diagonalize \mathcal{H}

$$\mathcal{H} = \sum_k \varepsilon_k (d_k^\dagger d_k - 1/2), \quad (\text{A11})$$

$$\varepsilon_k = 2\sqrt{1 + 2\mu \cos k + \mu^2}. \quad (\text{A12})$$

$\varepsilon_k > 0$ ensures that the ground state $|G\rangle$ is the vacuum $|0\rangle$ of the d_k .

2. Exact formulas for the spin probabilities

We define P_j^σ as the projector onto the $|\sigma = \pm 1\rangle_j^\zeta$ state

$$P_j^+ = c_j^\dagger c_j, \quad P_j^- = c_j c_j^\dagger. \quad (\text{A13})$$

p_i is then given by

$$p_i = p(\sigma_0, \dots, \sigma_{L-1}) = \langle 0 | P_0^\sigma P_1^\sigma, \dots, P_{L-1}^\sigma | 0 \rangle. \quad (\text{A14})$$

Using Wick's theorem, this correlator reduces to a Pfaffian. To compute it, we need to calculate the four types of contractions $\langle c_j^\dagger c_\ell \rangle$, $\langle c_j c_\ell^\dagger \rangle$, $\langle c_j^\dagger c_\ell^\dagger \rangle$, and $\langle c_j c_\ell \rangle$, which can be done using Eq. (A7). It is worth noticing that all these correlators are real in this particular model. We write a generic projector as

$$P_j^\sigma = f_j^\dagger f_j \quad (\text{A15})$$

with $f_j^\dagger = c_j^\dagger$ for $\sigma = +1$ and $f_j^\dagger = c_j$ for $\sigma = -1$. Then

$$p_i^2 = \langle f_0^\dagger f_0 f_1^\dagger f_1, \dots, f_{L-1}^\dagger f_{L-1} \rangle^2. \quad (\text{A16})$$

$$= \langle f_0^\dagger f_1^\dagger, \dots, f_{L-1}^\dagger f_0 f_1, \dots, f_{L-1} \rangle^2, \quad (\text{A17})$$

$$= \text{Pf}^2 \begin{pmatrix} A & B \\ -B & -A \end{pmatrix}, \quad (\text{A18})$$

where A is antisymmetric, B is symmetric, and Pf denotes the Pfaffian. The matrix elements of A and B are

$$A_{j\ell} = \langle f_j^\dagger f_\ell^\dagger \rangle, \quad \ell \geq j, \quad (\text{A19})$$

$$B_{j\ell} = \langle f_j^\dagger f_\ell \rangle. \quad (\text{A20})$$

Using the relation $\text{Pf}^2 = \det$, Eq. (A18) simplifies into

$$p_i^2 = \det \begin{pmatrix} A & B \\ -B & -A \end{pmatrix}, \quad (\text{A21})$$

$$= \det \begin{pmatrix} A+B & B \\ 0 & B-A \end{pmatrix}. \quad (\text{A22})$$

Equation (A22) follows from Eq. (A21) by adding the second column to the first and then the first row to the second. Finally,

$$p_i = \det(A+B) = \det M, \quad (\text{A23})$$

where M is a $L \times L$ matrix with elements

$$M_{j\ell} = \langle f_j^\dagger (f_\ell^\dagger + f_\ell) \rangle, \quad (\text{A24})$$

$$= \frac{1}{2} \delta_{j\ell} + \frac{\sigma_j^\zeta}{2L} \sum_k \cos[k(j-\ell) + 2\theta_k]. \quad (\text{A25})$$

At the critical point ($\mu=1$), $\theta_k = k/4$ and the matrix elements simplify even further

$$M_{j\ell} = \frac{1}{2} \delta_{j\ell} + \frac{(-1)^{j-\ell} \sigma_j^\zeta}{2L \sin[\pi(j-\ell + 1/2)/L]}. \quad (\text{A26})$$

¹L. Amico, R. Fazio, A. Osterloh, and V. Vedral, *Rev. Mod. Phys.* **80**, 517 (2008).

²S. Furukawa and G. Misguich, *Phys. Rev. B* **75**, 214407 (2007).

³D. S. Rokhsar and S. A. Kivelson, *Phys. Rev. Lett.* **61**, 2376 (1988).

⁴C. L. Henley, *J. Phys.: Condens. Matter* **16**, S891 (2004).

⁵J.-M. Stéphan, S. Furukawa, G. Misguich, and V. Pasquier, *Phys. Rev. B* **80**, 184421 (2009).

⁶This quantum/classical correspondence works in a rather straightforward way for simple constrained models (such as dimer models or vertex models). For other models, such as the Ising model considered in this paper, some additional care is needed to define the geometry of the A/B boundary at the microscopic level. In the particular case of 2D classical Ising models, the spins living at the frontier between A and B have to be “duplicated” to insure that the decomposition induced by the classical spin configurations is indeed a proper Schmidt decom-

position of the RK state. See Ref. 5 for more details.

⁷E. Fradkin and J. E. Moore, *Phys. Rev. Lett.* **97**, 050404 (2006).

⁸B. Hsu, M. Mulligan, E. Fradkin, and E.-A. Kim, *Phys. Rev. B* **79**, 115421 (2009).

⁹In the quantum point of view, where one studies the entanglement in a RK wave function, the dominant ($\sim L$) contribution is the boundary (also called “area”) law.

¹⁰The field-theory prediction of Ref. 8 is $r_1(T=T_c) = \ln(2)$ and does not agree with our numerical calculations. Remark: r_1 corresponds to $S_0^{(x)}$ in the notations of Ref. 5.

¹¹I. Affleck and A. W. W. Ludwig, *Phys. Rev. Lett.* **67**, 161 (1991).

¹² $T_c = 2/\ln(1+\sqrt{2})$ on the square lattice (Refs. 13 and 33) and $T_c = 4/\ln(3)$ on the triangular lattice (Ref. 34).

¹³H. A. Kramers and G. H. Wannier, *Phys. Rev.* **60**, 252 (1941).

¹⁴We also use the property that, for periodic boundary conditions, $\Pi_i \sigma_i^\zeta = 1$ in the ground state $|G\rangle$. Since we work in the σ^ζ basis,

- this reduces by another factor two the number of probabilities to compute.
- ¹⁵J. Sawada, *SIAM J. Comput.* **31**, 259 (2001).
- ¹⁶In fact, the analysis of Sec. IV C suggests that $r_n(\mu_c)$ flows to its ferromagnetic boundary condition limit, $\ln(2)$, as soon as $n > 1$.
- ¹⁷L. Campos Venuti, H. Saleur, and P. Zanardi, *Phys. Rev. B* **79**, 092405 (2009).
- ¹⁸R. J. Baxter, *Exactly Solved Models in Statistical Mechanics* (Dover, Mineola, 1982).
- ¹⁹S. Katsura, *Phys. Rev.* **127**, 1508 (1962).
- ²⁰M. Levin and X.-G. Wen, *Phys. Rev. Lett.* **96**, 110405 (2006).
- ²¹A. Kitaev and J. Preskill, *Phys. Rev. Lett.* **96**, 110404 (2006).
- ²²J. L. Cardy, *Nucl. Phys. B* **324**, 581 (1989).
- ²³J. Dubail, J. L. Jacobsen, and H. Saleur, *Nucl. Phys. B* **834**, 399 (2010).
- ²⁴M. A. Metlitski, C. A. Fuertes, and S. Sachdev, *Phys. Rev. B* **80**, 115122 (2009).
- ²⁵F. Gliozzi and L. Tagliacozzo, *J. Stat. Mech.: Theory Exp.* (2010), P01002.
- ²⁶The Rényi entropy can be computed for complex values of n and one can detect possible singularities by analyzing the locations of the its zeros in the complex plane, as was done in Ref. 25 for a different model. However, in our case, such an approach does not seem to shed more light on the $n=1$ issue than the real-axis analysis presented here.
- ²⁷See Eq. (77) in Ref. 5. We use the following normalization: $R = 1$ for free fermions and $R = \sqrt{2}$ at $SU(2)$ symmetric (self-dual) point of the XXZ chain. This corresponds to a Lagrangian $\mathcal{L} = \frac{1}{8\pi}(\partial_\mu \varphi)^2$, where the field is compactified on a circle of radius R : $\varphi = \varphi + 2\pi R$.
- ²⁸Mo. Oshikawa, [arXiv:1007.3789](https://arxiv.org/abs/1007.3789) (unpublished).
- ²⁹P. Calabrese and J. Cardy, *J. Stat. Mech.: Theory Exp.* (2004), P06002.
- ³⁰C. Holzhey, F. Larsen, and F. Wilczek, *Nucl. Phys. B* **424**, 443 (1994).
- ³¹V. B. Petkova and J.-B. Zuber, *Phys. Lett. B* **504**, 157 (2001).
- ³²M. Oshikawa and I. Affleck, *Phys. Rev. Lett.* **77**, 2604 (1996).
- ³³L. Onsager, *Phys. Rev.* **65**, 117 (1944).
- ³⁴R. Houtappel, *Physica (Amsterdam)* **16**, 425 (1950).